JCI The Journal of Clinical Investigation

A fibrin biofilm covers the blood clot and protects from microbial invasion

Fraser L. Macrae, … , Heiko Herwald, Robert A.S. Ariëns

J Clin Invest. 2018. https://doi.org/10.1172/JCI98734.

Research Article In-Press Preview **Hematology** **Vascular biology**

Haemostasis requires conversion of fibrinogen to fibrin fibres that generate a characteristic network, interact with blood cells, and initiate tissue repair. The fibrin network is porous and highly permeable, but the spatial arrangement of the external clot face is unknown. Here we show that fibrin transitioned to the blood-air interface through Langmuir film formation, producing a protective film confining the clot. We demonstrated that only fibrin is required to form the film, and that it occurred in vitro and in vivo. The fibrin film connected to the underlying clot network through tethering fibres. It was digested by plasmin and formation of the film was prevented with surfactants. Functionally, the film retained blood cells and protected against penetration by bacterial pathogens in a murine model of dermal infection. Our data show a remarkable aspect of blood clotting, in which fibrin forms a protective film covering the external surface of the clot, defending the organism against microbial invasion.

A fibrin biofilm covers the blood clot and protects from microbial invasion

Fraser L. Macrae[1†], Cédric Duval[1†], Praveen Papareddy[2], Stephen R. Baker[1], Nadira Yuldasheva[1], Katherine J. Kearney[3], Helen R. McPherson[1], Nathan Asquith[1], Joke Konings[4,5], Alessandro Casini[6], Jay L. Degen[7], Simon D. Connell[8], Helen Philippou[1], Alisa S. Wolberg[9], Heiko Herwald[2], Robert A. S. Ariëns[1,4,*]

Affiliations:

1. Thrombosis and Tissue Repair Group, Discovery and Translational Science Department, Leeds Institute of Cardiovascular and Metabolic Medicine, School of Medicine, University of Leeds, Leeds, UK.

2. Division of Infection Medicine, Department of Clinical Sciences, Faculty of Medicine, Lund University, Lund, Sweden;

3. Population and Clinical Sciences Department, Leeds Institute of Cardiovascular and Metabolic Medicine, School of Medicine, University of Leeds, Leeds, UK.

4. Department of Biochemistry, Cardiovascular Research Institute Maastricht, School of Medicine, University of Maastricht, Maastricht, the Netherlands

5. Synapse Research Institute, CARIM, University of Maastricht, Maastricht, the Netherlands.

6. Division of Angiology and Haemostasis, Faculty of Medicine, Geneva University Hospitals, Geneva, Switzerland.

7. Cincinnati Children's Hospital, Cincinnati, OH, USA

8. Molecular and Nanoscale Physics Group, School of Physics and Astronomy, University of Leeds, Leeds, UK.

9. Department of Pathology and Laboratory Medicine, University of North Carolina, Chapel Hill, NC, USA

† These authors contributed equally to this study.

The authors have declared that no conflict of interest exists.

*Correspondence to:
R A S Ariëns, PhD
LIGHT Laboratories
University of Leeds
Clarendon Way
Leeds, LS2 9JT
UK
Email: r.a.s.ariens@leeds.ac.uk
Tel: +44 113 343 7734.

Abstract: Haemostasis requires conversion of fibrinogen to fibrin fibres that generate a characteristic network, interact with blood cells, and initiate tissue repair. The fibrin network is porous and highly permeable, but the spatial arrangement of the external clot face is unknown. Here we show that fibrin transitioned to the blood-air interface through Langmuir film formation, producing a protective film confining the clot. We demonstrated that only fibrin is required to form the film, and that it occurred in vitro and in vivo. The fibrin film connected to the underlying clot network through tethering fibres. It was digested by plasmin and formation of the film was prevented with surfactants. Functionally, the film retained blood cells and protected against penetration by bacterial pathogens in a murine model of dermal infection. Our data show a remarkable aspect of blood clotting, in which fibrin forms a protective film covering the external surface of the clot, defending the organism against microbial invasion.

Introduction:

Haemostasis is a pivotal mechanism to prevent life-threatening blood loss from sites of injury, and involves close interplay between coagulation and platelets. The resulting blood clot contains activated platelets, red blood cells, and fibrin polymer which holds the clot together. Fibrin is formed by limited proteolysis of fibrinogen by thrombin. Thrombin cleaves small peptidic sequences from the N-termini of the Aα- and Bβ-polypeptides, exposing interaction sites for binding pockets in the C-terminal domains of the β- and γ-chains respectively (1). Fibrin thus polymerises into protofibrils, which aggregate laterally into fibres. The fibres branch and produce a three-dimensional network with remarkable elastic properties (2). The structure of the fibrin network is determined by fibre diameter, protofibril packing and pore size, the latter of which is sufficient for the incorporation of cells. Dense networks with thin fibres and increased rigidity are associated with increased risk of thrombosis, while loose clot networks with thick fibres and reduced rigidity are associated with bleeding (1, 3, 4).

A major conundrum after decades of fibrin polymer research is that fibrin fibres in the blood clot appear endless, with little evidence of fibre ends (Supplemental Figure.1). Thus, the mechanisms and structures that determine the external boundary of an extravascular (haemostatic) blood clot are unknown. What happens to the fibrin network and fibres when they reach the peripheral, exposed surface of the clot? Do the fibres just stop, flatten or bend, or is the surface lined by platelets, red blood cells or other cells? The architecture of this interface is important because it forms a distinction between host and the environment. To explore this, we investigated the structural characteristics of the exterior face of the blood clot, and found that fibrin at the blood-air interface is not arranged in the form of fibres, but instead transitions to a continuous sheet that covers the clot surface. This sheet arises through Langmuir film formation, provides a natural

limit to clot growth, prevents blood cell loss and protects from bacterial infection. These data reveal a novel critical role for fibrin in haemostasis through the generation of a previously unrecognized bio-protective film that encapsulates the clot in the early stages of tissue repair.

Results:

Film forms at air-liquid interface

Our study was motivated by observations from scanning electron microscopy (SEM) revealing a thin film on the clot surface where, prior to dehydration, the air-liquid interface had been. This film was present in clots formed from whole blood or platelet-poor plasma when clotting was initiated with thrombin (0.5 $U.ml^{-1}$; Figure.1A and B) or tissue factor (5 pM; Supplemental Figure.2A and B). Using laser scanning confocal microscopy (LSCM), we found the film was also present in clots from whole blood (thrombin - Figure.1C; tissue factor – Supplemental Figure.2C) and plasma (thrombin Figure.1D; tissue factor – Supplemental Figure.2D) in fully hydrated conditions. When single slices of a clot in the z-plane were imaged using LSCM, the film appeared continuous around the clot exterior (Figure.1E).

Film is composed of fibrin

Fluorescence detected in the LSCM images indicated fibrinogen or fibrin was present in the film (Figure.1C-E). To better characterise the film components, we peeled it away from the surface of plasma clots (Figure.2A) formed with or without T101 (transglutaminase inhibitor). The films were reduced and subjected to SDS-PAGE (Figure.2B). The film contained fibrin and this was confirmed by western blotting with a polyclonal antibody against fibrinogen (Supplemental Figure.3A).

To assess if the film could form from fibrin alone, we formed clots from purified fibrinogen (1 $mg.ml^{-1}$) and thrombin (0.5 $U.ml^{-1}$) and examined them using SEM and LSCM. We observed formation of films that mimicked those formed on whole blood and plasma clots (Figure.2C-D). Films transitioned to fibres in places (Figure.2E), and connected to the fibrin network through tethering fibres (Figure.2F). These observations show that fibrin(ogen) alone is capable of producing a film at the clot surface.

We next investigated how other plasma components influenced film formation. Purified fibrinogen was spiked with Alexa Fluor-488 fibrinogen (25μg.ml^{-1}) and different clotting conditions were tested. Film mean sheet fluorescence (MSF) and film thickness were measured to quantify changes (Supplemental Table.1).

The film formed at all thrombin concentrations (0.1, 0.5, 1, 10 U.ml^{-1}; Figure.2G, Supplemental Figure.3B). However, as the thrombin concentration increased, the MSF and film thickness of the film decreased in a stepwise manner, indicating a reduction in the quantity of fibrin present. Thrombin generation triggered by tissue factor in plasma starts slowly after a short lag-phase, and then its concentration rapidly increases to a maximum of several hundred nM (tens of U.ml^{-1}) (5, 6). However, fibrin formation occurs at just 2-3 nM thrombin (0.2-0.3 U.ml^{-1}), before the vast majority of thrombin has been generated (7). Our data indicates that the film forms most optimally at lower thrombin concentrations, which lead to longer clotting times allowing more fibrin to accumulate at the surface before the underlying network has formed. Previous data showed that lower thrombin concentrations are also optimal for maximum protofibril packing in fibrin fibres (8).

$CaCl_2$ concentration (5, 10, 20 mM) had no effect on film formation (Figure.2H, Supplemental Figure.3C), but the absence of $CaCl_2$ resulted in at least a 1.9x decrease in MSF and 1.5x decrease in film thickness. This indicates that film formation is not dependent on $CaCl_2$ concentration, but absence of $CaCl_2$ dramatically reduces its formation.

Film formation occurred at all fibrinogen concentrations tested (0.05, 0.5, 1, 2.5 mg.ml^{-1}, Figure.2I, Supplemental Figure.3D), even when the fibrinogen levels were not sufficient to form a clot that filled the whole volume of the liquid (Supplemental Figure.3E). Interestingly, as fibrinogen levels increased up to 1 mg.ml^{-1} the MSF and film thickness decreased in a stepwise manner signifying a decrease in film formation. Increases in fibrinogen concentration lead to

shorter lag times and faster clotting rates (9). So in a similar trend to thrombin concentrations, a shorter lag time led to less fibrin accumulating at the air-liquid interface leading to thinner films. We also investigated film formation in patients with dysfibrinogenemia and afibrinogenemia. To prevent changes in the clot or film structure with the addition of normal fluorescently labelled fibrinogen, a non-antibody binding protein (Affimer) (10) specific to fibrinogen was fluorescently labelled with Alexa fluor 488. This was then added to the patient plasma before clotting, where it bound to any fibrinogen within the plasma. A clot was then formed and imaged using LSCM (Supplemental Figure.3F). Patients with dysfibrinogenemia formed a film that had a higher MSF and thickness than clots formed from normal pool plasma. Afibrinogenemia patients did not form a fibrin clot or film as expected (Figure.2J).

Films were similar in clots produced with reptilase (2.4 $U.ml^{-1}$), which only cleaves fibrinopeptide A (and not B) from fibrinogen, and thrombin (Figure.2K, Supplemental Figure.3G). This demonstrates that film formation occurs during fibrinogen to fibrin conversion, regardless of the activating protease and independent of FpB release.

We also assessed the effect of temperature on film formation (21°C – room temperature, 31.5°C – skin temperature, 37°C – core body temperature). Although films formed at all three temperatures, film formation increased at least 20-30% at 31.5°C compared to room temperature or core body temperature (Figure.2L, Supplemental Figure.3H). Enhanced film formation at skin temperature is consistent with a physiological role for fibrin films in cutaneous wounds and dermal injuries.

There were no differences in film MSF or thickness with or without Factor XIII (FXIII) (3.7 $\mu g.ml^{-1}$; Figure.2M, Supplemental Figure.3I), showing that FXIII is not necessary for film formation.

The role of platelets in film formation was investigated by comparing film formation in platelet

poor (PPP) and platelet rich plasma (PRP). No difference in MSF and film thickness between PPP and PRP indicates that platelets do not influence film formation (Figure.2N, Supplemental Figure.3J).

To investigate whether fibrinogen structural elements are essential for film formation, we tested natural and recombinant fibrinogen variants: γA/γA, the common fibrinogen isoform; γA/γ', a heterodimeric splice variant which adds negative charge to the C-terminus of the γ-chain (11); γ3x, a triple γ-chain mutant (γ3x) that eliminates all γ-chain crosslinking (12); α220, in which the α-chain is truncated after residue Ser220 removing the connector and C-terminal globular domain of the αC-region; and α390, in which the α-chain is truncated after residue Asp 390 removing the C-terminal globular domain. Clots formed with each of these variants produced fibrin films (Figure.2O-Q, Supplemental Figure.4A-C). Differences in MSF were attributable to differences in polymerization rates and fibrin clot structure (13). These data indicate that neither the C-terminal domain of the γ-chain, the α-chain C-terminal connector region, nor the α-chain C-terminal globular domain are required for film formation.

Collectively, these findings show that fibrin produces a film that covers the blood clot at the air-liquid interface, and although other factors modulate film thickness or the amount of fibrin in the film, only fibrin is required.

Mechanism of film formation

The transition of film to fibres (Figure.2E) and connection of film to the clot network via tethering fibres (Figure.2F) indicated that a specific biophysical mechanism governs fibrin film formation. To identify this mechanism, we used LSCM to visualise film formation and breakdown in plasma and purified fibrinogen solutions. Clot formation was initiated with thrombin (0.5 $U.ml^{-1}$) in plasma (Figure.3A, Supplemental Movie.1) or purified fibrinogen (Supplemental Figure.4D, Supplemental Movie.2), and with tissue factor (5 pM) in plasma

(Supplemental Figure.4E, Supplemental Movie.3). Fibrin accumulated at the surface forming a film before, or at a similar rate as the earliest fibrin fibres that constitute the clot network underneath. Once the clot was fully formed, breakdown was initiated with tPA (85 $ng.ml^{-1}$) in plasma clots, or tPA plus plasminogen (25 $\mu g.ml^{-1}$) in purified systems, and observed over time (plasma - Figure.3B, Supplemental Movie.4; purified – Supplemental Figure.4F, Supplemental Movie.5). In both cases, the films lysed at approximately the same rate as the network of fibrin fibres.

We next investigated accumulation of fibrinogen and fibrin at the air-liquid interface using a Langmuir-Blodgett trough, which analyses monolayer film formation of amphiphilic molecules at the air-liquid interface (14, 15). Few previous studies have investigated fibrinogen at the air-liquid interface (16-19), and none have examined fibrin. Purified fibrinogen or fibrin monomers (fibrinogen ± 1 $U.ml^{-1}$ thrombin and 5 mM GPRP) were injected into the sub-phase of the trough at increasing quantities (1 $x10^{13}$ – 100 $x10^{13}$ molecules of fibrinogen/fibrin) and surface pressure measurements were recorded over time. As protein accumulated at the surface over time, surface pressure increased and then plateaued, resulting in a maximum pressure (Figure.3C). At 1 $x10^{13}$ molecules neither fibrin nor fibrinogen covered the surface so there was no increase in surface pressure. At 5 and 20 $x10^{13}$ molecules of fibrinogen/fibrin there was a delay before fibrinogen or fibrin resulted in an increase in surface pressure. But higher quantities (30 and 100 $x10^{13}$ molecules) of fibrinogen and fibrin caused an increase in surface pressure almost instantaneously (Figure.3C inserts, Supplemental Table.2). Maximum surface pressure escalated with increasing amounts of fibrinogen and fibrin (Figure.3C-D, Supplemental Table.3). Fibrin presented with significantly lower surface pressures than fibrinogen at 5 and 20 $x10^{13}$ molecules, but as the quantity of fibrinogen/fibrin increased, these differences were no longer seen. The addition of more than 30 $x10^{13}$ molecules of fibrinogen did not further increase maximum pressure (100

$x10^{13}$ and 5312 $x10^{13}$ molecules (1 $mg.ml^{-1}$)), signifying that 30 $x10^{13}$ (0.006 $mg.ml^{-1}$) is the maximum amount of fibrin/fibrinogen that can be accommodated at the surface. This was much lower than physiological fibrinogen levels (2-4 $mg.ml^{-1}$). From this we calculated that this would allow for ~34 nm^2 per fibrin/fibrinogen molecule. Assuming a fibrin(ogen) D-region is ~6.5-6.7 and the E-region is ~5-5.3 nm in diameter (20, 21) the half-staggered fibrin model (22) would allow for ~31-34 nm^2 per fibrin/fibrinogen molecule, in close agreement with our experimental data. This indicates that fibrin/fibrinogen molecules are tightly packed and are positioned perpendicularly to the air-liquid interface.

In order to investigate the morphology of the film below the surface we compared the interior and the exterior surfaces using SEM. The film was peeled away from the exterior of the clot and stretched over a coverslip with either the interior or exterior surface exposed (Figure.3E). The exterior surface was smooth, sometimes with very small pores (~24.8 ± 8.8 nm pores, yellow arrows) or with small nodes (~6.4 ± 0.9 nm domains, yellow circles). In contrast, the interior surface was rough with holes, pores and a fibrous structure, more closely resembling the clot network. In agreement with the Langmuir-Blodgett trough data, these data imply that fibrin films have an ordered, dense structure at the surface, but become less ordered deeper in the film where they transition into more fibrous structures.

With the interior surface looking similar to a clot network, we hypothesised that fibrin polymerisation was involved in film formation. To assess this, we followed the accumulation of fibrin/fibrinogen below the surface and analysed the effects of polymerization over time using LSCM. Time courses of polymerizing fibrin, fibrin monomers or fibrinogen alone spiked with Alexa Fluor-488 fibrinogen were followed in a purified (1 $mg.ml^{-1}$ fibrinogen/fibrin) or plasma system (2x dilution). Accumulation was quantified by MSF (Figure.3F-G). Purified fibrinogen accumulated at the air-liquid surface with a maximum rate of 0.26 ± 0.03 $MSF.min^{-1}$, reaching

maximum fluorescence (5.5 ± 1.3 MSF) after 57.3 ± 2.1 min. Fibrin monomers had a maximum rate ~3-fold faster than that of fibrinogen (0.8 ± 0.8 MSF.min^{-1}), with twice as much protein accumulating at the surface (Max MSF – 10.4 ± 0.8) after 58 ± 1.5 min. Polymerizing fibrin accumulated at the surface at the greatest rate, with a maximum increase in fluorescence of 1.46 ± 0.39 min^{-1}, over 5-fold the rate of fibrinogen. It reached a maximum fluorescence (27.1 ± 1.1 MSF) after 59 ± 0.7 min (Figure.3F-G, Supplemental Figure.5A, Supplemental Table.4 and Supplemental Movie.2, 6 and 7). The same pattern was seen in plasma with polymerizing fibrin accumulating at the surface quicker than fibrin monomers and fibrinogen (Supplemental Figure.5B-D, Supplemental Table.4 and Supplemental Movie.1, 8 and 9). This indicates that fibrin polymerization contributes to film formation by enhancing the accumulation of fibrin at the air-liquid interface. This effect is likely due to a combination of stronger interactions between the molecules of fibrin versus fibrinogen, and an increase in hydrophobicity of fibrin (1, 23), which retains it at the surface.

We next investigated film strength using atomic force microscopy (AFM). Young's Modulus was calculated for plasma samples with and without transglutaminase inhibitor T101 by fitting a Sneddon model for conical tips to all force curves found over the entire area that was imaged (Supplemental Figure.6A-B). Fibrin fibres were visible under the film surface and these areas presented with much stiffer Young's modulus than places suspended between fibres. To find the stiffness of the film alone, Young's Modulus was determined by measuring areas between the underlying fibres of clots formed from plasma. The average Young's Modulus of the film was ~3-fold lower than regions supported by fibres (suspended- 7.65 ± 0.24 kPa vs fibre - 21.79 ± 2.79 kPa, p=0.0001). Inhibition of cross-linking decreased the modulus of the suspended film further by just over 10-fold to 0.72 ± 0.14 kPa, which is slightly more than the decrease in fibrin stiffness previously reported in whole clots and single fibres (2-8.5x) (24-27). Areas supported

by fibrin fibres decreased just over 4-fold to 5.1 ± 0.75 kPa in the absence of cross-linking (Supplemental Figure.6C). As a consequence, although fibrin crosslinking is not required for film formation (Figure.2L), it increases film elastic modulus.

Given that fibrin accumulates at the air-liquid interface, we hypothesised that film formation should be preventable by blocking the air interface with surfactant molecules. Accordingly, addition of tween-20 (0.1%) prevented film formation and resulted in a dense, partly collapsed clot, probably due to the loss of surface tension (Figure.3H). Furthermore, blocking the air-liquid interface using mineral oil or petroleum jelly also prevented film formation (Supplemental Figure.6D).

Based on the Langmuir (Figure.3C-D) and accumulation data (Figure.3F-G) we propose a model (Figure.4A) where, upon injury and exposure to air, fibrinogen molecules in the blood are rapidly adsorbed to the air exposed surface, forming an organized monolayer at the air-liquid interface. Simultaneously, tissue factor stimulates fibrinogen cleavage via thrombin, leading to fibrin formation. Fibrin(ogen) continues to rise and accumulate at the air-liquid interface, packing in more molecules. At the same time fibrin begins to fit together in a half-staggered formation, allowing for the build-up of multiple layers of fibrin through A:a knob-hole interactions, and the formation of tethering fibres (Figure.4A-C). This leads to a dense layer of fibrin across the surface of the clot.

Protection against microbes

In view of the rapid formation of the fibrin film after exposure to an air-interface, we hypothesised that an important physiological role of the film is to form an immediate barrier to protect the vascular breach against microbial invasion until white blood cells are recruited to the wound site.(28) To investigate this hypothesis, we used a Boyden chamber to analyse migration of three types of bacteria commonly found in the natural skin flora (*Escherichia coli*,

Staphylococcus epidermidis and *Staphylococcus aureus)* through clots (Figure.5A). Bacteria were grown to 3.6-8.5 x10^8 cells.ml^{-1}, fluorescently-labelled with *Bac*Light green, and applied to the external surface of three types of clots: 1) clots formed with 0.1% tween-20 to prevent film formation, 2) clots where the surface was perforated with a needle to make holes in the film and 3) normal clots with intact film. Fluorescent bacteria that moved through the clots were quantified over 48 hours (Figure.5B, Supplemental Figure.7A). The time taken for the first bacteria to break through the clots was defined as when fluorescence became greater than 2% of the total added fluorescent bacteria. No fluorescent bacteria migrated through the clots within the first 8 hours. *E. coli* migrated through the perforated (11.3 ± 1.2 hours) and tween-20 treated clots (25.3 ± 1.2 hours) significantly faster than the normal clots (38.0 ± 7.2 hours) (Figure.5C; p=0.0008). A similar trend was seen with the two other bacteria (Supplemental Figure.7B). After the initial breakthrough, rate of bacteria migration was comparable between clot types. This suggests the film prevents bacterial infiltration into the site of injury for at least 12-27 hours, allowing time for white blood cell recruitment and the underlying clot to fully form.

Fibrin film formation in vivo and blood cell retention

To investigate the role of the film on bacteria migration in vivo, we established a novel murine dermal injury model. Initially, we investigated if fibrin film formation occurred ex vivo in mouse blood. Clots were formed with whole blood from wildtype (WT) or fibrinogen-deficient mice and were prepared for SEM. Blood from WT mice formed a fibrin film at the air-liquid interface, whereas blood from fibrinogen-deficient mice did not (Supplemental Figure.8A). We next established a murine dermal injury model in which a 2 mm puncture was created in the skin on the back or abdomen of anaesthetised mice. The injury was either left clear to clot exposed to the air or immediately covered with a thin layer of oil to remove the air-liquid interface, which was

washed off with saline once the clot had formed. After 60 minutes, clots and surrounding skin were surgically removed, processed, and imaged by SEM (Figure.6A). In the untreated control section, clots possessed a film on the exterior surface. Consistent with the in vitro experiments, oil treatment prevented film formation, leaving the fibrous fibrin network exposed and clearly visible by SEM (Figure.6A). Some of these clots were embedded in paraffin, sectioned, and stained using Marcius, Scarlet and Blue (MSB) or were probed with a fibrin specific antibody (59D8). In the untreated control sections the film can be seen along the surface of the clot, as a thin pink layer with MSB (Figure.6B), or a thin brown layer with 59D8, confirming that fibrin makes up the film in vivo (Supplemental Figure.8B). In clots treated with oil, the film is not present. This showed that the oil prevented film formation in vivo and could be used to assess bacterial migration and proliferation in clots without a film.

During the establishment of our in vivo model, we found histology sections of clots formed in the presence of oil – and therefore lacking the film – showing regions of loose cells that were not retained within the clot (Figure.6C). In micrographs of the control clots we found erythrocytes pushed against the inside of the film (Figure.6D). These findings suggested the fibrin film helps to prevent leakage of blood cells from dermal lesions. To investigate this, we formed clots from whole blood either with no intervention, in the presence of tween-20 (0.1 %) or with the film being perforated after 1 hour. After two hours the amount of haemoglobin released from the clot was measured. We found that the quantity of haemoglobin released was more than 12-fold higher in the tween (4.37 ± 0.38 g.L^{-1}) and perforated clots (4.14 ± 0.85 g.L^{-1}), with almost no haemoglobin being released from the normal clot (0.32 ± 0.18 g.L^{-1}, $p=0.0002$, Figure.6E). This data shows that the film plays a role in the retention of red blood cells within the clot.

Protective role of fibrin film in a murine dermal injury model

We next investigated the role of the fibrin film in protection against bacterial proliferation and dissemination in vivo. After the clots were formed as described above (with or without a layer of oil), 2 µl of bioluminescent *Pseudomonas aeruginosa* (4 x10^5 CFU), a Gram-negative flagellated bacterium associated with severe hospital-acquired infections and significant resistance to antibiotics, were carefully deposited on the surface of the clots covering the dermal punctures. Mice were imaged every 4h using a three dimensional IVIS spectrum in vivo imaging system to assess bacterial proliferation. Control experiments were run in parallel to demonstrate oil had no effect on bacterial proliferation. In the mice with an intact fibrin film the bioluminescence did not increase over 12 hours, showing that the bacteria did not proliferate over this period in these mice (Figure.7A-B, Supplemental Table.5). In contrast, in mice without a fibrin film the bioluminescence was significantly higher after 4h and increased over time up to 103400 $p^{-1}.sec^{-1}.cm^{-2}.sr^{-1}$ (IQR - 46950, 358750), compared to 0.1505 $p^{-1}.sec^{-1}.cm^{-2}.sr^{-1}$ (IQR - 0.1065, 0.3713, p=0.0005) in the mice with films (Figure.7A-B, Supplemental Table.5). These data show that the bacteria were proliferating within the wound in the absence of the film. To confirm the difference in bacteria numbers, the clots and surrounding skin were harvested from sacrificed animals after 12 hours and mechanically homogenised. Serial dilutions of the homogenates were plated on agar to analyse bioluminescence and bacterial CFUs (Figure.7C-D). In agreement with the bioluminescence data, the mice that had no film on their clot showed a much greater number of bacteria (2.53 ± 0.298 x10^6 $CFU.ml^{-1}$) within the wound and skin than the mice that had an intact clot film (0.064 ± 0.014 x10^6 $CFU.ml^{-1}$). These data demonstrate that the film has a protective role, slowing or preventing the proliferation of bacteria and reducing the movement of bacteria into wounds and skin in the first 12 hours after injury.

Discussion:

This study demonstrates that fibrin has a hitherto undisclosed and entirely unexpected role in haemostasis, producing a film that not only encapsulates the clot and thereby retains cells, but also functions as a protective layer at the interface between the clotting blood and the air, preventing microbial infection. The structural characteristics of this fibrin film are completely different from that of the fibrin fibre network. The film is composed of a thin continuous layer of fibrin and is connected to the fibrous fibrin network through tethering fibres. Film formation is initiated by the exposure of blood to the air-interface, and accumulates due to the conversion of fibrinogen to fibrin, and the resultant increase in hydrophobicity of the fibrin molecule (1, 23). The unique fibrin polymerisation mechanisms, which involves knob-hole interactions, leads to fibrin being able to produce both films and fibres (29), and we show that this culminates in a remarkable integrated clot structure that includes a fibrin film covering a network of fibres. This new finding transforms our understanding of blood clots at injury sites and sheds new light on a major enigma of how the clot ends at the air-blood interface which has troubled the field for a long time.

The film has previously been observed in our laboratory and that of others in SEM images of blood, plasma or fibrin clots. However, until now, it has been overlooked, as it was alleged to be an artefact of sample preparation. The close association of fibrin clot structure with thrombosis risk (3, 30, 31), has lead researchers to focus on areas of the clot not covered by the fibrin film, *i.e.* away from the clot air-interface, or in areas where the film may have ruptured during sample processing. Previous studies have shown that fibrin is able to produce sheet-like structures, across gaps in a striated substrate for example (29) or in blood clots (32). However, the physiological relevance of these structures and the mechanism of formation were never explored.

Here, we investigated the film in detail, and found it to be a physiological product of clotting and fibrin formation.

Fibrinogen and fibrin have previously been associated with protection against systemic infection (33, 34). Our new data demonstrate that fibrin additionally plays an important role in controlling local infection at injury sites, forming an instant barrier that slows the proliferation of bacteria and delays its movement into the wound, allowing the underlying clot to fully form and create a more permanent barrier. A lack of this clot barrier film is expected to lead to a significant increase in infection. Our data indicate that future studies are required into the use of petroleum jelly to help stem bleeds from injuries in contact sports, or to a wound after minor surgery. Another area of clinical interest is afibrinogenemia, since the lack of fibrin film formation in this disease may lead to increased risk of persistent infections from minor dermal lesions (Supplemental Figure.9). As per corollary, an engineered fibrin film would be expected to improve recovery from minor and major injuries and reduce the probability of severe infection.

Our findings of the extraordinary formation of a protective fibrin film on the blood clot exterior show a unique novel mechanism in haemostasis that helps retain blood cells and control microbial infection. Clot film formation appears an important physiological process, which should be exploited in the future to improve recovery and healing from minor and major injuries.

Methods

Materials

Human plasma fibrinogen, plasminogen-depleted (Calbiochem; Nottingham, UK), was further purified by immunoaffinity chromatography (IF-1 mAb, 10mg; Kamiya Biomedical; Seattle, USA) as previously described (35), to eliminate FXIII (36). AlexaFluor-488 or -594 fibrinogen (Invitrogen; Paisley, UK) was reconstituted to 2.5 $mg.ml^{-1}$, human thrombin (Calbiochem; Nottingham, UK) was reconstituted to 250 $U.ml^{-1}$, tissue plasminogen activator (tPA; Pathway Diagnostics; Dorking, UK) and Glu-plasminogen (Enzyme Research Laboratories, Swansea, UK) were diluted in 0.05 M Tris-Base, 0.1 M NaCl, pH 7.4 (TBS) to 1 $mg.ml^{-1}$ and 990 $\mu g.ml^{-1}$, respectively, and stored at –80°C. Human FXIII-A_2B_2 was isolated from contaminating albumin and glucose from Fibrogammin P (Zedira; Darmstadt, Germany) by Sepharose-6B gel filtration as described (12). FXIII was diluted in TBS to 110 $\mu g.ml^{-1}$ and stored at –80°C. All other chemicals were obtained from Sigma-Aldrich (Gillingham, UK) unless stated otherwise.

Whole blood

Samples of free-flowing blood were collected from the antecubital vein of healthy volunteers. Blood was collected on 0.109 M sodium citrate and the blood was used within 4 hours.

Platelet poor and platelet rich plasma

Free-flowing blood was obtained from the antecubital vein of 24 healthy volunteers as described above. The blood was centrifuged at 2,400 g for 20 minutes for platelet poor plasma (PPP), or at 200 g for 10 minutes for platelet rich plasma (PRP). PPP and PRP from 6 individuals were used to form clots for film formation comparison. PPP samples from 24 volunteers were pooled, aliquoted, and snap-frozen in liquid nitrogen and stored at -80˚C.

Purification of γA/γA and γA/γ' fibrinogen

γA/γA and γA/γ' fibrinogens were isolated as previously described (8, 37, 38). In short, the variants were separated using a DE-52 column on the AKTAavant 25 (GE Healthcare, Amersham, UK). Fibrinogen was dissolved in 39 mM Tris, 65 mM H_3PO_4, 0.5 mM phenylmethylsulfonyl fluoride (PMSF), 1 mM benzamidine and 5 mM ε-aminocaproic acid, pH 8.6. Samples were eluted using a concave gradient from 0% to 100% over 13 column volumes (with increments of 5% over the first 6 and increments of 10% over the next 7 column volumes) of 500 mM Tris, 650 mM H_3PO_4, 0.5 mM PMSF, 1 mM benzamidine and 5 mM ε-aminocaproic acid, pH 4.2. The fibrinogens were concentrated and dialysed in 50 mM Tris-HCl and 100 mM NaCl pH 7.4. The purity of the γA/γA and γA/γ' preparations was checked on a NuPAGE unit with 4-12% Bis-Tris gradient gels (Invitrogen, Paisley, UK), and aliquots were stored at -80°C.

Mutant fibrinogen expression

Recombinant human fibrinogen expression and purification has been described previously (12, 35). Briefly, truncations (αSer220 and αAsp390) and γ-chain mutations (Q398N/Q399N/K406R referred to as γ3x) were established through the use of QuikChange II Site-Directed Mutagenesis Kit (Agilent Technologies; Stockport, UK*).* The expression vector pMLP encoded the entire cDNA for either the α- or γ-chain. Primers were designed to change residues at desired locations (γ398, 399, 406) or to create a stop codon at α221 and α391. Mutations and truncations were confirmed by sequencing (MRC PPU DNA Sequencing and Services; University of Dundee, Scotland). Plasmids were transfected into Chinese hamster ovarian (CHO) cells containing the remaining fibrinogen chains. A second plasmid was transfected for selection (pMSV-his). Recombinant fibrinogen WT, γ3x and α-truncations were produced in roller bottles containing

microcarrier beads and DMEM/F12 (Thermo Fisher Scientific; Paisley, UK), medium was supplemented with aprotinin, 5 $\mu g.ml^{-1}$ insulin, 5 $\mu g.ml^{-1}$ transferrin and 5 $ng.ml^{-1}$ sodium selenite (Roche; Welwyn Garden City, UK). Medium was collected and replaced every 48 hours and stored at -40 °C with the addition of 150 μM PMSF, and harvested for 8 weeks. The fibrinogen was precipitated overnight with 40% saturated ammonium sulphate (VWR International, Leicestershire, UK) and a mixture of protein inhibitors (MES hydrate 20 mM pH 5.6, 6-Aminihexanoic acid 5 mM, benzamidine 5 mM, PMSF 100 μM, pepstatin 1 μM, leupeptin 1 μM). The precipitated medium was centrifuged at 14,500 g for 45 minutes without brakes at 4°C in an Avanti J-265 XPI (Beckman Coulter, High Wycombe, UK). The pellet was re-suspended in a protein cocktail (NaCl 333 mM, Tris 222 mM, PMSF 111 μM, pepstatin 5 μM, leupeptin 5 μM, EDTA 1 mM, trypsin inhibitor 11 $U.mL^{-1}$, benzamidine 5 mM, 6-Aminihexanoic acid 5 mM), incubated for 30 min at 4 °C and centrifuged at 43,000 g for 30 minutes. Supernatant was collected and kept at -80 °C. Samples were purified by immunoaffinity chromatography (IF-1 mAb, 10 mg; Kamiya Biomedical; Seattle, USA) as previously described (35). Fractions containing fibrinogen were pooled and stored at –80°C. Fibrinogen was concentrated and dialysed in 50 mM Tris-HCl and 100 mM NaCl pH 7.4. Protein integrity was assessed by SDS-PAGE.

Scanning electron microscopy – whole blood, plasma, purified, thrombin/tissue factor

Clots for scanning electron microscopy (SEM) were prepared by adding 10 μl of activation mixture (Whole blood/plasma – human thrombin 0.5 $U.ml^{-1}$ or tissue factor 5 pM (Diagnostica Stago; Theale, UK), $CaCl_2$ 5 mM, Purified fibrinogen – human thrombin 0.5 $U.ml^{-1}$, $CaCl_2$ 5 mM final concentrations, in TBS) to 100 μl of whole blood, plasma or purified fibrinogens ± FXIII (final concentrations: Fibrinogen – 1 $mg.ml^{-1}$, FXIII – 3.7 $\mu g.ml^{-1}$). The clotting mixture was

immediately transferred to pierced Eppendorf lids. Clots were left to form in a humidified chamber at room temperature for 2 hours. Clots were washed with saline solution to remove excess salt and prepared for microscopy by fixation in 2 % glutaraldehyde solution for at least 120 minutes. Clots were further washed with sodium cacodylate buffer (67 mM $C_2H_6AsNaO_2$, pH 7.4) and dehydrated in a series of increasing acetone concentrations (30–100 %). Clots were critical-point dried with CO_2, mounted onto stubs and sputter-coated with platinum using a Cressington 208 HR (Cressington Scientific Instruments, Watford, UK). Each clot was formed in duplicate and imaged in five areas, at different magnifications (2500, 5000, 10000, 20000, 25000 and 50000) using a Hitachi SU8230 high performance cold field emission (CFE) SEM (Chiyoda, Tokyo, Japan).

Laser scanning confocal microscopy – whole blood, plasma and purified

Reaction mixtures were prepared by diluting whole blood or plasma by half with saline or TBS respectively, and spiked with 25 $\mu g.ml^{-1}$ AlexaFluor-594 fibrinogen or -488 respectively and 5 mM $CaCl_2$. 0.5 $U.ml^{-1}$ of human thrombin or 5 pM tissue factor was added to initiate clotting. Purified fibrinogen (1 $mg.ml^{-1}$) was spiked with 25 $\mu g.ml^{-1}$ AlexaFluor-488 fibrinogen, with or without FXIII (3.7 $\mu g.ml^{-1}$) and 5 mM $CaCl_2$. 0.5 $U.ml^{-1}$ of human thrombin was added to initiate clotting. Immediately after the initiation of clotting a 30 µl drop of the mixture was transferred to the centre of the well of an uncoated 8-well Ibidi slide (Ibidi GmbH, Munich, Germany) and the slide was transferred to a dark humidity chamber for 4 hours at room temperature. Imaging was performed using an inverted Zeiss LSM880 microscope (Carl Zeiss; Welwyn Garden City, UK) with a 40× oil immersion objective lens. Fibrin clots were prepared in duplicate and four images were taken at the air-liquid interface for each clot (Supplemental Figure.10A), Z-stacks

(20 μm, 30 slices) were combined to form 3D images (ZEN 2.1 black, Carl Zeiss, Cambridge, UK).

Conditions - thrombin, calcium, fibrinogen concentration, reptilase, temperature, platelets, fibrinogen variants.

LSCM and SEM were carried out as above, but with changes to some of the conditions. Experiments were carried out in which clotting was initiated with different thrombin (final concentrations: 0.1, 0.5, 1, 10 $U.ml^{-1}$), $CaCl_2$ concentrations (0, 5, 10, 20 mM) and fibrinogen concentrations (0.05, 0.5, 1, 2.5 $mg.ml^{-1}$) in a purified system. Clotting was also initiated with reptilase (2.4 $U.ml^{-1}$; Diagnostica Stago; Theale, UK) to investigate the effects of only cleaving fibrinopeptide A compared to thrombin ($0.5U.ml^{-1}$).

The effects of temperature were investigated by incubating the reaction mix at different temperatures (21 °C, 31.5 °C, 37 °C) before and throughout clotting. Average skin temperature was determined as 31.5 °C using a contact thermometer on the fore-arm and hand. Immediately after clotting initiation, a 30 μl drop of the reaction mixture was transferred into the centre of the well of an uncoated 8 well Ibidi slide (Ibidi GmbH) and the slide was transferred to a dark humidity chamber in an incubator at the appropriate temperature for 4 hours.

The effects of platelets on film formation were studied by comparing film formation between platelet poor plasma and platelet rich plasma from 6 healthy volunteers. Reaction mixtures were prepared by diluting PPP or PRP by half with saline, and spiked with 25 $\mu g.ml^{-1}$ AlexaFluor-594 fibrinogen and 5 mM $CaCl_2$. 5 pM tissue factor was added to initiate clotting.

The effects of fibrinogen variants were investigated with purified γA/γA or γA/γ', γ3x mutant, α220 or α390 mutants (each at 2.94 μM).

Fibrin(ogen)-binding Affimers for imaging the film in dys- and afibrinogeneamia

Free-flowing blood was obtained from the antecubital vein of 2 dysfibrinogenemia patients (FGA c.112A>G - p.R38G, FGG c.901C>T - p.R301C) and 3 afibrinogenemia patients (FGA c.635T>G - p.L212X, FGA c.635T>G - p.L212X, FGA c.635T>G - p.L212X) as described above. The blood was centrifuged at 2,400 g for 20 minutes for PPP. These samples were aliquoted, and snap-frozen in liquid nitrogen and stored at -80˚C. To image the plasma samples a fibrin(ogen) specific Affimer was isolated from an Affimer phage display library using a previously described screening process (10). This Affimer was fluorescently labelled using an Alexa Fluor 488 protein labelling kit (Invitrogen, Carlsbad, California, United States) according to manufacturer's instructions. Fluorescently labelled Affimer was then added to normal pool plasma or patient plasma at 17.6 μM and incubated for 30 mins. Clotting was initiated with 5 mM CaCl2 and 0.5 U.ml-1 of human thrombin and a 30 μl drop of the mixture was immediately transferred to the centre of the well of an uncoated 8-well Ibidi slide (Ibidi GmbH, Munich, Germany). Clots were incubated for 4 hours in a humidity chamber and were then imaged by LSCM as previously described.

Confocal time series formation/lysis

To investigate film formation, the reaction mixture was produced as above for both plasma and purified fibrinogen. A 27 μl drop of this mixture was placed into the centre of a well of an uncoated 8-well Ibidi slide (Ibidi GmbH, Martinsried, Germany) of thrombin (0.5 $U.ml^{-1}$) or tissue factor (5 pM) was added to the drop which was immediately observed by LSCM. The effects of preventing polymerization were investigated by pre-incubating fibrinogen (1 $mg.ml^{-1}$) or plasma with GPRP (5 mM) for 20 min. 3 μl of thrombin (0.5 $U.ml^{-1}$) was added to the drop,

which was immediately observed by LSCM using a 40x oil immersion objective lens with 29 x 0.7 µm z-stacks every 60 seconds.

To investigate fibrinolysis, clots were formed as mentioned above. After film formation, 5 µl of tPA (85 $ng.ml^{-1}$) was added to plasma clots, and 5 µl of plasminogen (25 $\mu g.ml^{-1}$) and tPA (85 $ng.ml^{-1}$) was added to purified clots. The clot was immediately observed by LSCM. Formation and lysis were observed by LSCM using a 40x oil immersion objective lens. 29 x 0.7 µm z-stacks were obtained every 60 seconds. 3D videos were created from the z-stacks.

Preventing film formation – oil, tween-20, petroleum jelly

The reaction mixture was made up for plasma as mentioned above for reactions with oil or petroleum jelly. For oil experiments, mineral oil was carefully placed around the drop to fill the confocal well before clotting, to eliminate the air-liquid interface before clotting was initiated. For petroleum jelly experiments, 27 µl of reaction mixture was injected into a small ball of petroleum jelly that had been placed in the middle of the well of a slide. For reactions with tween-20, the reaction mix was incubated with 0.1 % tween-20 before clotting. Using a pipette, thrombin (0.5 $U.ml^{-1}$) was added to the reaction mixture to initiate clotting. The slide was transferred to a humidity chamber for 4 hours at room temperature. Imaging was performed using an inverted Zeiss LSM880 microscope with a 40× oil immersion objective lens. Each fibrin clot was prepared in duplicate and four images were taken of each sample, Z-stacks were combined to form 3D images.

Film thickness

To measure film thickness, the thickness of the film was measured on confocal images 60 times per image using Image J (v2.0, NIH), and the average thickness for each image was used to compare between conditions.

Fluorescence measurements

To quantify film fluorescence, an outline was drawn around the film on each focal plane. Area, integrated density and three adjacent background readings were made using ImageJ (v2.0, NIH). The corrected film fluorescence = integrated density – (area selected × mean fluorescence of background readings). This was calculated for each focal plane. The average of the corrected film fluorescence of each focal plane was taken and was divided by 10,000 arbitrarily to simplify the numbers, and was called Mean Sheet Fluorescence (MSF). To validate this method, measurements of film thickness from confocal images of 72 separate samples were taken. 60 measurements of film thickness were taken per image using ImageJ, and the average thickness for each image was correlated with MSF taken from the same image (Supplemental Figure.10B).

Film peel

Clots were generated by spreading 100 µl of plasma ± 1,3,4,5-Tetramethyl-2-[(2-oxopropyl)thio]imidazolium chloride (T101, FXIII inhibitor, 1 mM; Zedira; Darmstadt, Germany) or purified fibrinogen (1 $mg.ml^{-1}$) ± FXIII (3.7 $\mu g.ml^{-1}$) into an approximately 2x2 cm square on coverslip. 10 µl of activation mixture (human thrombin, 0.5 $U.ml^{-1}$ and $CaCl_2$ 5 mM) was added to initiate clotting. After 4 hours a hypodermic needle was used to peel the film away from the surface of the clot (Figure.2A). The film was either reduced and run on SDS-PAGE, or it was stretched over a coverslip exposing either the interior surface or exterior surface of the film and was prepped for SEM.

SDS-PAGE and western blot

Clots were made using plasma by the addition of thrombin (0.5 $U.ml^{-1}$) and $CaCl_2$ (5 mM), with and without FXIII inhibitor T101 (1 mM). The fibrin film was removed from each clot and reduced by the addition of NuPAGE sample reducing agent (100 mM DTT) and heating at 95 °C for 15 minutes. Fibrin sample was prepared by the formation of a clot with IF-1 fibrinogen (1 $mg.ml^{-1}$) and addition of thrombin and $CaCl_2$, and reduction as described above. FXIII, Bovine Serum Albumin (BSA) and IF-1 purified fibrinogen samples were reduced in a similar way, and run alongside the films to help identify bands in the gel, and as controls for the blots. Protein concentrations were determined using Nanodrop, to load 2 μg of each protein sample on two identical 4-12 % NuPAGE bis-tris gels. After running, one gel was stained using GelCode Blue Safe Protein Stain (Thermo Scientific, Paisley, UK) and one was transferred to a PVDF membrane (Thermo Scientific). The membrane was blocked overnight using 4% skimmed milk in 50 mM Tris, 150 mM NaCl, 0.1 % tween-20. Polyclonal rabbit anti-human fibrinogen antibody (A0080; Dako, Ely, UK) was added to the blot in blocking buffer, and detected using goat anti-rabbit-HRP secondary antibody (P0448; Dako). Signal was detected using Supersignal West Pico Chemiluminescent Substrate (Thermo Scientific).

Atomic Force Microscopy sample preparation

Samples for AFM mechanical measurements and imaging were prepared from normal pool plasma with a one in two final dilution. Briefly, plasma was mixed with an activation mix of $CaCl_2$ (5 mM) and thrombin (0.5 $U.ml^{-1}$) and placed onto 34 mm diameter tissue culture dish (TPP, Trasadingen, Switzerland) with the plasma mixture covering a 10x10 mm square. For samples with T101, a final concentration of 1 mM was added to the mixture. Samples were then

placed into a humidity chamber and allowed to clot for 1 hour. Samples were hydrated with 3-5 ml of 50 mM Tris, 100 mM NaCl and placed on the AFM sample stage. Imaging and force measurements were performed on a JPK NanoWizard 4 and a Zeiss AxioObserver D1 in qi mode with 10 nm radius AFM probes (CB3, qp-BioAC, Nanosensors, Neuchâtel, Switzerland). All measurements were done in triplicate over a 15x15 μm square.

Langmuir-Blodgett trough

Surface tension measurements were used to determine fibrinogen and fibrin adsorption at the air-liquid interface. Measurements were performed with an extra small KSV NIMA double barrier Langmuir-Blodgett trough (203 x 50 x 1.2 mm) with surface pressure sensor, based on the Wilhelmy method, with a Whatman CHR1 chromatography paper plate (perimeter 20.6 mm; accuracy in surface pressure - 0.01 $\mu N.m^{-1}$; KSV NIMA, Biolin Scientific, Manchester, UK). Because adsorption measurements are sensitive to the presence of impurities, extreme care was taken to ensure that all materials and instruments used in this study were clean. The trough and barriers were cleaned with methanol and rinsed with deionized water before each run. A new Wilhelmy plate was used for each run. Due to the duration of the experiment, the trough was maintained in a dust and draught exclusion cabinet throughout the measurements to minimise the presence of impurities from the atmosphere. A humid atmosphere was maintained by putting a trough of water in the enclosing box. The sub-phase was composed of 30 ml of 0.2 μm filtered TBS pH 7.4 at room temperature. The surface was checked prior to each measurement to ensure that it was clean by moving the barriers to the centre and confirm that the surface pressure was below 0.3 $mN.m^{-1}$. The system was set to record surface pressure every second for 18 hours. The desired protein concentration was achieved by diluting in TBS (fibrinogen – 1, 5, 20, 30, 100, 5312 $x10^{13}$ molecules (final concentrations - 0.00018 – 1 $mg.ml^{-1}$); fibrin 1, 5, 20, 30, 100 $x10^{13}$

molecules (final concentrations - 0.00018 - 0.019 $mg.ml^{-1}$)), and was injected into the sub-phase in one 50 µl injection with a Hamilton gastight syringe (Thermo Scientific), and was left for 18 h. Fibrin monomers were formed by pre-incubating fibrinogen with GPRP (5mM) overnight, followed by incubation with thrombin (0.5 $U.ml^{-1}$) for 2 hours. As a control a 50 µl mixture of thrombin (0.5 $U.ml^{-1}$) and GPRP (5 mM) was run on the trough to show that it caused no change in surface pressure.

Bacteria migration assay

To investigate bacteria migration, an assay was set up using a Boyden chamber (VWR, Lutterworth, UK) shown in Figure.5A. Three types of bacteria, *Escherichia coli* (ATCC #13706), *Staphylococcus epidermidis* (ATCC #12228) and *Staphylococcus aureus* (ATCC #29247), commonly found in the natural skin flora were transformed with pSELECT-Zeo plasmid (Invivogen, Toulouse, France) to provide resistance to antibiotic Zeocin. A single colony was picked for each bacterium and was grown up overnight (3.6-8.5 $x10^8$ $cells.ml^{-1}$) in nutrient broth containing Zeocin (25 $\mu g.ml^{-1}$, Sigma-Aldrich). Three clots for each strain of bacteria were formed in a Boyden chamber (0.8 µm pores, Millipore, Billerica, MA), two normal (Fibrinogen – 1 $mg.ml^{-1}$, $CaCl_2$ – 5 mM, Thrombin – 0.5 $U.ml^{-1}$) and one in the presence of tween-20 (0.1 %) and left overnight in a humidity chamber at room temperature. The next day the film on one of the normal clots for each bacterium was perforated by running a hypodermic needle across the surface of the clot. Each bacterium was fluorescently labelled with *Bac*Light green following manufacturer's instructions (ThermoFischer Scientific, Ulm, Germany). The bacteria were then spun down and re-suspended in 50% nutrient broth to remove any unused label, and were checked for fluorescence levels. Zeocin (25 $\mu g.ml^{-1}$) was added to SOC media (Thermo Fisher), and 1 ml was added to each well of the plate. Each clot was placed in the well and 300 µl of labelled bacteria was added in the chamber on top of each clot. 50 µl of SOC

media was taken from each well and replaced with fresh SOC media every 2 hours for 48 hours and measured for fluorescence. The time to the first bacteria breaking through the clots was defined as when fluorescence became greater than 2 % of the added fluorescent bacteria.

Ex vivo wildtype and fibrinogen deficient mouse clots

C57BL/6 and fibrinogen-deficient mice (C57BL/6 background; in house) (39), aged nine- to fourteen-week old and weighing 19-30 g were used for all experiments (n=4). Male and female mice were used in equal numbers. The mice were anaesthetized with isoflurane and bled through the IVC on 0.109 M sodium citrate before being euthanized. Whole blood clots from WT and fibrinogen-deficient mice were prepared for scanning electron microscopy (SEM) as described above, but clotting was initiated with mouse thrombin (0.5 $U.ml^{-1}$). Each clot was formed in duplicate and imaged in five areas, at 5 different magnifications (2500, 5000, 10000, 25000 and 50000×) using a Hitachi SU8230 high performance cold field emission (CFE) SEM (Chiyoda, Tokyo, Japan).

In vivo mouse dermal punctures

C57BL/6 (in house) or BALB/cJRj (Janvier Labs; Le Genest-Saint-Isle, France), aged nine- to fourteen-week old and weighing 19-30 g were used for all experiments. Male and female mice were used in equal numbers. The mice were anaesthetized with isoflurane, the abdomen was shaved and waxed. Six puncture wounds were created using a 2 mm biopsy punch (World Precision Instruments Ltd, Hitchin, UK), and were filled with blood from a tail vein. The injury was either left clear or immediately covered with a thin layer of oil to remove the air-liquid interface. After 60 min the animals were euthanized by cervical dislocation, the area around the wound together with the clot for each condition was surgically removed and fixed in 4 %

paraformaldehyde (histology or immunohistochemistry, n=4) or 2 % glutaraldehyde (SEM, n=4). The fixed tissues were dehydrated and embedded in paraffin. Consecutive 5 μm sections were cut and mounted. Sections were then stained with Martius, Scarlet and Blue (MBS) to observe the sectioned wound, collagen appears in blue, erythrocytes in yellow and fibrin in pink. Slides were observed under an Olympus BX40 Dual View microscope, and photographs were taken using Image Pro-Plus 8.0 software. For immunohistochemistry an EXPOSE rabbit specific HRP/DAB detection IHC kit (ab80437, Abcam, Cambridge, UK) was used following manufacturer's instructions. Slides were stained with mouse anti-fibrin antibody (59D8, 1:1000, antibody provided by Charles Esmon, Oklahoma Medical Research Foundation, Oklahoma City, Oklahoma, USA), which detects mouse fibrin (40) for 1 hour at room temperature in a humidity-controlled chamber. The sections were washed and incubated with HRP-conjugated anti-mouse secondary antibody. Negative controls were stained simultaneously in the absence of primary antibody. Alternatively after fixing, samples were prepared for SEM as described above for clots.

Red blood cell retention assay

Red blood cell retention was measured by analysing the quantity of haemoglobin released from different types of whole blood clots. Whole blood clots were formed in a well of an uncoated 8-well Ibidi slide (Ibidi GmbH, Martinsried, Germany), in the presence of $CaCl_2$ (5 mM), with the addition of 1 pM tissue factor and incubated in a humidity chamber for 2 hours at room temperature. Clots were either formed with no intervention, in the presence of tween-20 (0.1 %) or with the film being perforated after 1 hour. After 2 hours saline solution was added to the clot surface and the clots were placed on an orbital shaker (400 rpm) for 30 mins. A sample of the solution above the clot surface was carefully taken and was diluted by 50 % in distilled water

and left for 30 mins for haemolysis to occur. The samples were then analysed for haemoglobin levels using the Harboe method and a spectrophotometer (41).

Wound infection model

Bioluminescent *P. aeruginosa* (strain Xen 41, derived from the parental pleural isolate PAO1; PerkinElmer, Waltham, MA), possessing a copy of the luxCDABE operon of *P. luminescens*, integrated at a single site on the chromosome, were aerobically grown in Todd Hewitt (TH) broth at 37 °C to logarithmic phase (OD_{620}~0.5). Bacteria were harvested, washed in PBS, and diluted in the same buffer to 2 $x10^8$ colony forming units $CFU.ml^{-1}$.

BALB/cJRj mice (8 weeks of age; Janvier Labs; Le Genest-Saint-Isle, France) were maintained under specific-pathogen-free conditions and had free access to commercial chow and water. Male and female mice were used in equal numbers. For the experimental procedures, animals were anaesthetised with isoflurane, and one puncture wound was created using a 2 mm biopsy punch (World Precision Instruments Ltd, Hitchin, UK) on the back of each mouse. The puncture wound was filled with blood, from a BALB/cJRj donor mouse, and the wound was either left to clot while exposed to the air for 30 min (experimental group 1, n=8), or immediately covered with mineral oil and left to clot for 30 min, before the oil was washed off the clot with saline (experimental group 2, n=8). As a control to investigate the effect of oil on bacterial proliferation, blood was not added to the puncture wounds on some mice, and these were either left untreated (control group 1, n=4) or covered with mineral oil (control group 2, n=4). All animals were subsequently infected with 2 µl of bioluminescent *P. aeruginosa* suspension carefully deposited on top of the clots. Mice were then anaesthetized and imaged to check that the same amount of bacteria was added to each mouse and then anaesthetized again at 4, 8, 12 hours after bacterial infection to allow for data acquisition using a three-dimensional IVIS

Spectrum In Vivo Imaging System (PerkinElmer), and analysis using the Living Image® software (PerkinElmer). Differences in appearance between mice +film and –film in Figure.7 are due to the oil used to prevent film formation being transferred to the fur of the mice.

Determination of bacterial colony forming units

In order to study bacterial growth and dissemination, the skin around the wound was harvested from sacrificed animals at the end of the experiment (12 hours). The tissues were mechanically homogenized using 1.4 mm ceramic beads (Qiagen; Sollentuna, Sweden) and a MagNA Lyser (Roche; Bromma, Sweden), and serial dilutions were subsequently plated on TH agar plates overnight at 37 °C in order to enumerate the bacterial CFU present in the samples.

Statistics and software

All statistical analyses were performed with GraphPad Prism7. All experiments were repeated at least three times. Data was tested for normality using Shapiro-Wilk normality test. Data are presented as mean and standard deviation (SD) for parametric data and mean and interquartile range (IQR) for non-parametric data. For the comparisons of two groups, a two-tailed unpaired *t*-test was performed. For comparisons between multiple groups either a one-way ANOVA followed by a Dunnett's multiple comparisons test or a two-way ANOVA for parametric data was performed and a Kruskal-Wallis test for non-parametric data. A p-value less than 0.05 was considered significant.

Study approval

Ethical approval for blood taking was obtained from the University of Leeds Medical School or the University Hospitals of Geneva and Faculty of Medicine review board. Written informed

consent was received from each patient and volunteer prior to inclusion in the study in accordance with the declaration of Helsinki. Written informed consent was provided for picture provided in Supplemental Figure.9. All mouse experiments were conducted according to institutional guidelines and were authorized by either the University of Leeds Ethics Committee, in accordance with Home Office UK Animals (Scientific Procedures) Act 1986 or Malmö-Lund Animal Care Ethics Committee, Sweden (entry no. M89-16).

Contributions:

F.L.M. and R.A.S.A. conceived the project. F.L.M., R.A.S.A., C.D., P.P., S.R.B., K.J.K., J.K., A.C., S.D.C., H.P., A.S.W and H.H. contributed to design of the project, discussion and interpretation of results. F.L.M. performed most of the experiments unless stated otherwise. C.D. and H.R.M performed mutant fibrinogen expression. C.D., P.P and N.Y. designed and performed murine experiments. S.R.B designed, performed and analysed AFM experiments. K.J.K. performed Affimer experiments, SDS-PAGE and Western blot experiments. S.D.C and N.A. helped design and perform Langmuir-Blodgett trough experiments. A.C provided dysfibrinogenemia and afibrinogenemia patient samples. J.D. provided fibrinogen deficient mice. F.L.M., C.D. and R.A.S.A. wrote the manuscript. All authors critically reviewed the manuscript.

Acknowledgments:

This work was supported by the British Heart Foundation (RG/13/3/30104, RASA and PG/16/60/32292, RASA), the Knut and Alice Wallenberg Foundation (2011.0037, HH), the Swedish Foundation for Strategic Research (SB12-0019, HH) and the Swedish Research Council (2016-01104, HH). We thank A. Winkel for assistance with AFM measurements at JPK instruments. We also thank M. Fuller (Faculty of Biological Sciences, University of Leeds) for SEM sample preparation.

References and Notes:

1. Weisel, J.W. 2005. Fibrinogen and fibrin. *Adv Protein Chem* 70:247-299.
2. Liu, W., Jawerth, L.M., Sparks, E.A., Falvo, M.R., Hantgan, R.R., Superfine, R., Lord, S.T., and Guthold, M. 2006. Fibrin fibers have extraordinary extensibility and elasticity. *Science* 313:634.
3. Undas, A., and Ariëns, R.A. 2011. Fibrin clot structure and function: a role in the pathophysiology of arterial and venous thromboembolic diseases. *Arterioscler Thromb Vasc Biol* 31:e88-99.
4. Wolberg, A.S. 2010. Plasma and cellular contributions to fibrin network formation, structure and stability. *Haemophilia* 16 Suppl 3:7-12.
5. Hemker, H.C., and Beguin, S. 1995. Thrombin generation in plasma: its assessment via the endogenous thrombin potential. *Thromb Haemost* 74:134-138.
6. Hemker, H.C., Giesen, P., Al Dieri, R., Regnault, V., de Smedt, E., Wagenvoord, R., Lecompte, T., and Beguin, S. 2003. Calibrated automated thrombin generation measurement in clotting plasma. *Pathophysiol Haemost Thromb* 33:4-15.
7. Brummel, K.E., Paradis, S.G., Butenas, S., and Mann, K.G. 2002. Thrombin functions during tissue factor-induced blood coagulation. *Blood* 100:148-152.
8. Domingues, M.M., Macrae, F.L., Duval, C., McPherson, H.R., Bridge, K.I., Ajjan, R.A., Ridger, V.C., Connell, S.D., Philippou, H., and Ariëns, R.A. 2016. Thrombin and fibrinogen gamma' impact clot structure by marked effects on intrafibrillar structure and protofibril packing. *Blood* 127:487-495.
9. Weisel, J.W., and Nagaswami, C. 1992. Computer modeling of fibrin polymerization kinetics correlated with electron microscope and turbidity observations: clot structure and assembly are kinetically controlled. *Biophys J* 63:111-128.
10. Tiede, C., Bedford, R., Heseltine, S.J., Smith, G., Wijetunga, I., Ross, R., AlQallaf, D., Roberts, A.P., Balls, A., Curd, A., et al. 2017. Affimer proteins are versatile and renewable affinity reagents. *Elife* 6.
11. Macrae, F.L., Domingues, M.M., Casini, A., and Ariëns, R.A. 2016. The (Patho)physiology of Fibrinogen gamma'. *Semin Thromb Hemost* 42:344-355.
12. Standeven, K.F., Carter, A.M., Grant, P.J., Weisel, J.W., Chernysh, I., Masova, L., Lord, S.T., and Ariëns, R.A. 2007. Functional analysis of fibrin {gamma}-chain cross-linking by activated factor XIII: determination of a cross-linking pattern that maximizes clot stiffness. *Blood* 110:902-907.
13. McPherson, H., Duval, C., Asquith, N., Domingues, M.M., Baker, S., Ridger, V.C., Connell, S., Philippou, H., Ajjan, R., and Ariëns, R. 2017. Role of Fibrinogen αC Domain in Fibrin Fibre Lateral Aggregation and αC Connector Region In Longitudinal Fibre Growth; Complex Interactions of the αC Region that Regulate Clot Structure and Function. In *Congress of the International Society on Thrombosis and Haemostasis*. Berlin: Res Pract Thromb Haemost. 1-1451.
14. Hann, R.A. 1990. Molecules for Langmuir-Blodgett-Film Formation. *Philos Trans R Soc Lond A* 330:141-152.

15. Langmuir, I. 1917. The Shapes of Group Molecules Forming the Surfaces of Liquids. *Proc Natl Acad Sci U S A* 3:251-257.

16. Hernandez, E.M., and Franses, E.I. 2003. Adsorption and surface tension of fibrinogen at the air/water interface. *Colloids Surf A Physicochem Eng Asp* 214:249-262.

17. Razumovsky, L., and Damodaran, S. 1999. Surface activity-compressibility relationship of proteins at the air-water interface. *Langmuir* 15:1392-1399.

18. Sankaranarayanan, K. 2015. Role of viscogens on the macromolecular assemblies of fibrinogen at liquid/air and solid/air interfaces. *Biointerphases* 10:021009.

19. Sankaranarayanan, K., Dhathathreyan, A., and Miller, R. 2010. Assembling fibrinogen at air/water and solid/liquid interfaces using Langmuir and Langmuir-Blodgett films. *J Phys Chem B* 114:8067-8075.

20. Ciesla, M., Adamczyk, Z., Barbasz, J., and Wasilewska, M. 2013. Mechanisms of fibrinogen adsorption at solid substrates at lower pH. *Langmuir* 29:7005-7016.

21. Hall, C.E., and Slayter, H.S. 1959. The fibrinogen molecule: its size, shape, and mode of polymerization. *J Biophys Biochem Cytol* 5:11-16.

22. Fowler, W.E., Hantgan, R.R., Hermans, J., and Erickson, H.P. 1981. Structure of the fibrin protofibril. *Proc Natl Acad Sci U S A* 78:4872-4876.

23. van Oss, C.J. 1990. Surface properties of fibrinogen and fibrin. *J Protein Chem* 9:487-491.

24. Collet, J.P., Shuman, H., Ledger, R.E., Lee, S., and Weisel, J.W. 2005. The elasticity of an individual fibrin fiber in a clot. *Proc Natl Acad Sci U S A* 102:9133-9137.

25. Helms, C.C., Ariëns, R.A., Uitte de Willige, S., Standeven, K.F., and Guthold, M. 2012. alpha-alpha Cross-links increase fibrin fiber elasticity and stiffness. *Biophys J* 102:168-175.

26. Liu, W., Carlisle, C.R., Sparks, E.A., and Guthold, M. 2010. The mechanical properties of single fibrin fibers. *J Thromb Haemost* 8:1030-1036.

27. Shen, L., and Lorand, L. 1983. Contribution of fibrin stabilization to clot strength. Supplementation of factor XIII-deficient plasma with the purified zymogen. *J Clin Invest* 71:1336-1341.

28. Velnar, T., Bailey, T., and Smrkolj, V. 2009. The wound healing process: an overview of the cellular and molecular mechanisms. *J Int Med Res* 37:1528-1542.

29. O'Brien, E.T., 3rd, Falvo, M.R., Millard, D., Eastwood, B., Taylor, R.M., 2nd, and Superfine, R. 2008. Ultrathin self-assembled fibrin sheets. *Proc Natl Acad Sci U S A* 105:19438-19443.

30. Ariëns, R.A. 2016. Novel mechanisms that regulate clot structure/function. *Thromb Res* 141 Suppl 2:S25-27.

31. Bridge, K.I., Philippou, H., and Ariëns, R. 2014. Clot properties and cardiovascular disease. *Thromb Haemost* 112:901-908.

32. Pretorius, E., Oberholzer, H.M., van der Spuy, W.J., Swanepoel, A.C., and Soma, P. 2012. Scanning electron microscopy of fibrin networks in rheumatoid arthritis: a qualitative analysis. *Rheumatol Int* 32:1611-1615.

33. Prasad, J.M., Gorkun, O.V., Raghu, H., Thornton, S., Mullins, E.S., Palumbo, J.S., Ko, Y.P., Hook, M., David, T., Coughlin, S.R., et al. 2015. Mice expressing a mutant form of fibrinogen that cannot support fibrin formation exhibit compromised antimicrobial host defense. *Blood* 126:2047-2058.

34. Degen, J.L., Bugge, T.H., and Goguen, J.D. 2007. Fibrin and fibrinolysis in infection and host defense. *J Thromb Haemost* 5:24-31.

35. Duval, C., Allan, P., Connell, S.D., Ridger, V.C., Philippou, H., and Ariëns, R.A. 2014. Roles of fibrin alpha- and gamma-chain specific cross-linking by FXIIIa in fibrin structure and function. *Thromb Haemost* 111:842-850.

36. Hethershaw, E.L., Cilia La Corte, A.L., Duval, C., Ali, M., Grant, P.J., Ariëns, R.A., and Philippou, H. 2014. The effect of blood coagulation factor XIII on fibrin clot structure and fibrinolysis. *J Thromb Haemost* 12:197-205.

37. Wolfenstein-Todel, C., and Mosesson, M.W. 1981. Carboxy-terminal amino acid sequence of a human fibrinogen gamma-chain variant (gamma'). *Biochemistry* 20:6146-6149.

38. Cooper, A.V., Standeven, K.F., and Ariëns, R.A. 2003. Fibrinogen gamma-chain splice variant gamma' alters fibrin formation and structure. *Blood* 102:535-540.

39. Suh, T.T., Holmback, K., Jensen, N.J., Daugherty, C.C., Small, K., Simon, D.I., Potter, S., and Degen, J.L. 1995. Resolution of spontaneous bleeding events but failure of pregnancy in fibrinogen-deficient mice. *Genes Dev* 9:2020-2033.

40. Hui, K.Y., Haber, E., and Matsueda, G.R. 1983. Monoclonal antibodies to a synthetic fibrin-like peptide bind to human fibrin but not fibrinogen. *Science* 222:1129-1132.

41. Cookson, P., Sutherland, J., and Cardigan, R. 2004. A simple spectrophotometric method for the quantification of residual haemoglobin in platelet concentrates. *Vox Sang* 87:264-271.

Figures

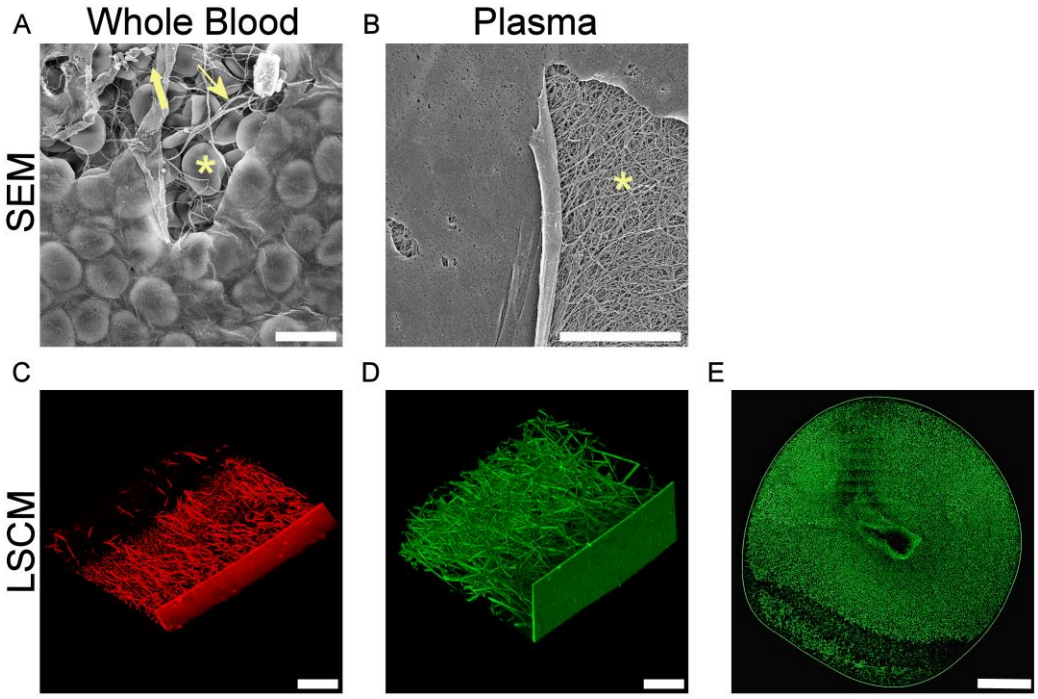

Figure. 1. **Film forms on the clot surface at the air-liquid interface**. **A**, **B**, SEM of film formed at the air-liquid interface in whole blood and plasma clots. At places where the film is torn (due to SEM sample processing procedures), red blood cells (asterisk), platelets (thick arrow) and fibrin (thin arrow) are observed in whole blood clots, and fibrin in plasma clots. Red blood cells are also seen shining through the film in whole blood clots. **C**, **D**, LSCM of film formed at the air-liquid interface in whole blood and plasma clots. Fibrinogen was fluorescently labelled with Alexa Fluor-488 (green) or -594 (red). Under fully hydrated conditions of LSCM, tears in the film were not observed. **E.** LSCM of a single z-plane slice of a plasma clot showing continuous film around the clot. The central gap in the clot image is where the pipette was introduced into the plasma drop to inject thrombin. Images represent findings reproduced in at least n=3 experiments. Scale bars: A, B – 10μm, C, D - 50μm, E - 1mm. All images representative of n=3 experiments.

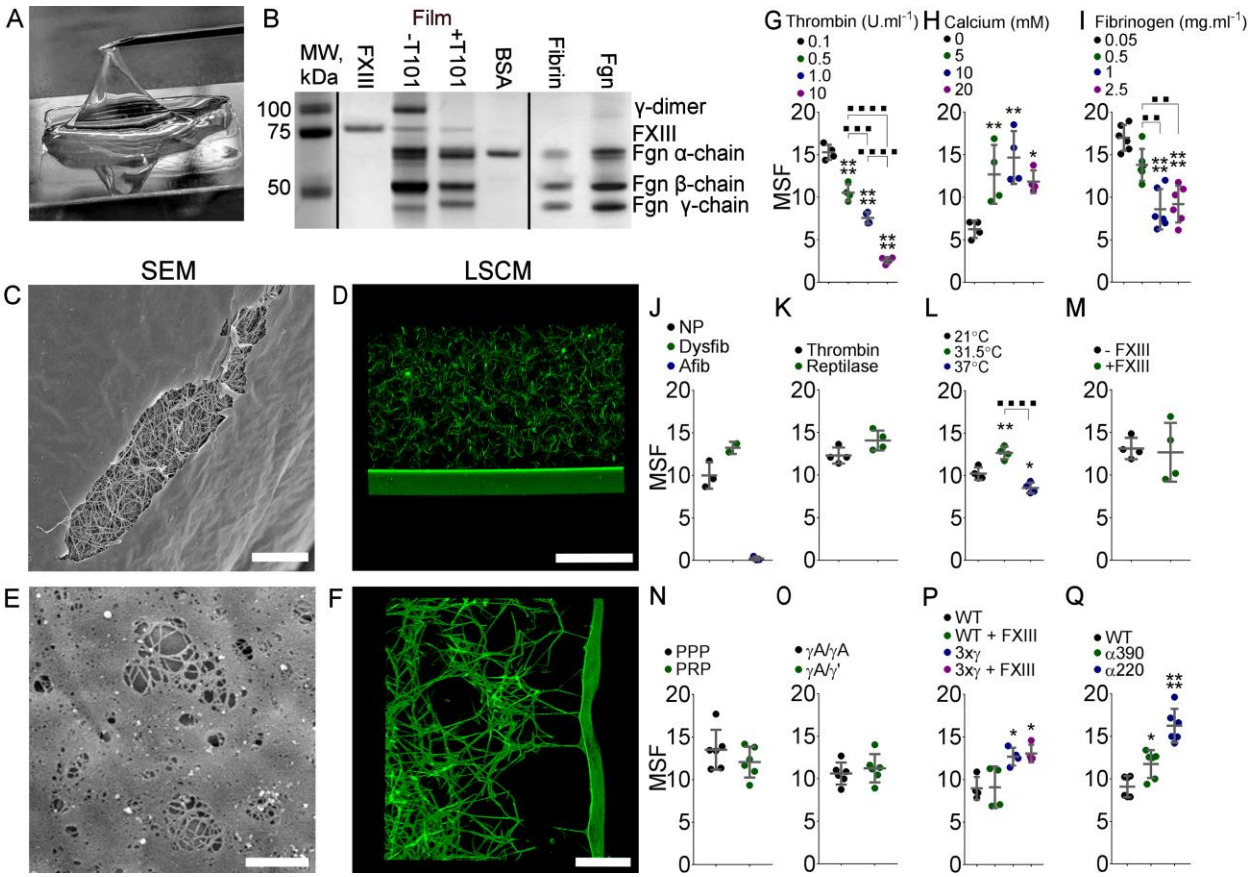

Figure. 2. Film only requires fibrin to form A, The film was peeled from clots using a needle. **B,** Films removed from clots produced ±T101 were run alongside FXIII, BSA, purified fibrin and purified fibrinogen (Fgn), on reducing SDS-PAGE. MW – molecular weight marker. **C**, SEM of the film in a clot produced from purified fibrinogen. A tear in the film exposes the underlying clot as often observed in SEM. Scale bar - 10µm. **D**, LSCM of the film at the air-liquid interface of a clot produced from purified fibrinogen, without breaks in fully hydrated conditions. Fibrinogen fluorescently labelled with Alexa Fluor-488. Scale bar - 50µm. **E,** SEM image of areas of film transitioning into fibres. Scale bar - 1µm. **F**, LSCM of tethering fibres connected to the film. Scale bar - 50µm. Images A-F representative of n=3 experiments. **G-Q,** Mean sheet fluorescence (MSF) measurements of the film comparing different conditions – **G**, thrombin concentration, n=4 experiments, **H**, $CaCl_2$ concentration, n=4 experiments, **I**, Fibrinogen concentration, n=6 experiments, **J**, Normal pool (NP, n=3 patients) v Dysfibrinogenemia (Dysfib, n=2 patients)/Afibrinogenemia (Afib, n=3 patients), **K**, thrombin v reptilase, n=4 experiments, **L**, temperature, n=4 experiments, **M**, Factor XIII (FXIII), n=4 experiments, **N**, Platelet poor plasma (PPP) v Platelet rich plasma (PRP), n=6 individuals, **O**, γA/γA fibrinogen v γA/γ' fibrinogen, n=6 experiments , **P**, fibrinogen triple γ-chain crosslinking mutant, n=6 experiments, **Q**, fibrinogen α-chain deletion mutants, n=6 experiments. * represents difference from 1st column, ▪ represents difference between other columns. * $p<0.05$, ** or ▪▪ $p<0.01$, *** or ▪▪▪ $p<0.001$, **** or ▪▪▪▪ $p<0.0001$. Mean ± SD. Unpaired t-test (two groups); ANOVA (multiple groups). FXIII – factor XIII, Fgn – fibrinogen, Dysfib – Dysfibrinogenemia, Afib – Afibrinogenemia, WT – Wildtype.

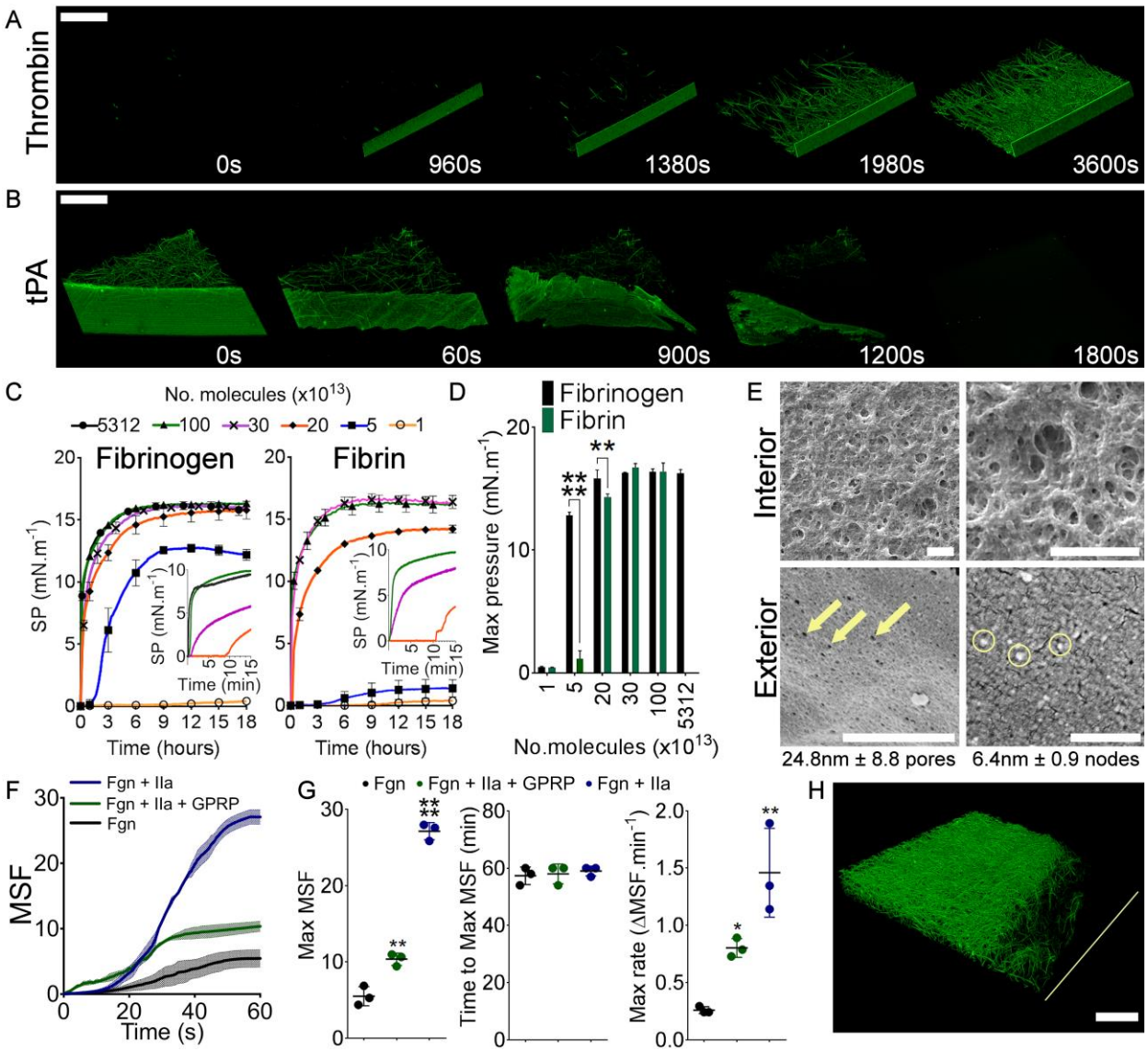

Figure. 3. Mechanism of fibrin film formation. **A**, Stills from movies of fibrin film formation over time in plasma when clotting is initiated with thrombin (n=3 experiments). Scale bar - 50µm. **B**, Stills from movies of film lysis by tPA in plasma (n=3 experiments). Scale bar - 50µm. **C**, Changes in surface pressure in the Langmuir-Blodgett trough with different fibrinogen or fibrin concentrations over time. Inserts show early time points (0-15min). Data shown as mean ± SD, n=3 experiments, SP – Surface pressure. **D**, Maximum Langmuir-Blodgett trough surface pressure of fibrinogen and fibrin with increasing concentrations, data shown as mean ± SD, ** $p<0.01$, **** $p<0.0001$, n=3 experiments, 2-way ANOVA, F= 293.5, df=1, p=<0.0001. **E**, SEM images of the interior and exterior surfaces of films peeled away from plasma clots. Note differences in scale bars – Interior 3µm, Exterior left 500nm, right 50nm. **F,** Accumulation of MSF of clots from purified fibrinogen over time analysed by LSCM, data shown as mean ± SD. **G**, Maximum MSF, n=3 experiments, F=330.7, df=2, p=< 0.0001, time to maximum MSF, n=3 experiments, F=0.1875, df=2, p=0.8337, maximum rate of MSF increase, n=3 experiments, F=20.55, df=2, p=0.0021 as analysed by LSCM, data shown as mean ± SD. * represents difference from black bar, * $p<0.05$, ** $p<0.01$, **** $p<0.0001$. **H**, LSCM image of the air-liquid interface of a plasma clot formed in the presence of tween-20 (0.1%), eliminating the film covering the clot. Yellow line represents the location of the air-liquid interface. Image representative of n=3 experiments. Scale bar - 50µm. MSF – mean sheet fluorescence, Fgn – fibrinogen, IIa – thrombin, GPRP – Gly-Pro-Arg-Pro peptide.

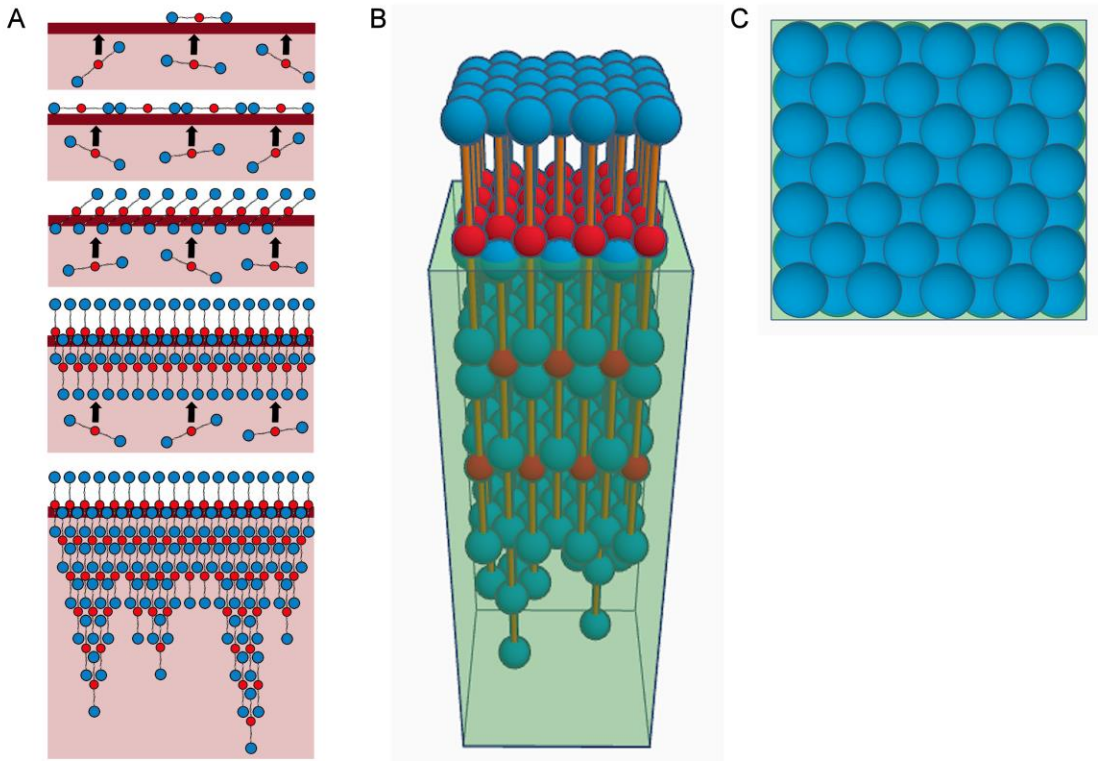

Figure. 4. A model of fibrin film forming at the clot surface. **A,** Proposed 2D model of fibrin(ogen) rising to the air-liquid interface and accumulating into a multi-layer film with half-staggered fibrin molecules and tethering protofibrils (beginning of fibrin fibres). **B,** A side-on view of a 3D model of the fibrin film with half-staggered fibrin molecules. D-regions are represented by 6.7nm diameter blue spheres, E-regions are represented by 5.3nm diameter red spheres and the connecting α-, β- and γ-chains are represented by an orange cylinder. The translucent box represents the liquid at the air-liquid interface **C,** Top view of the 3D fibrin film model.

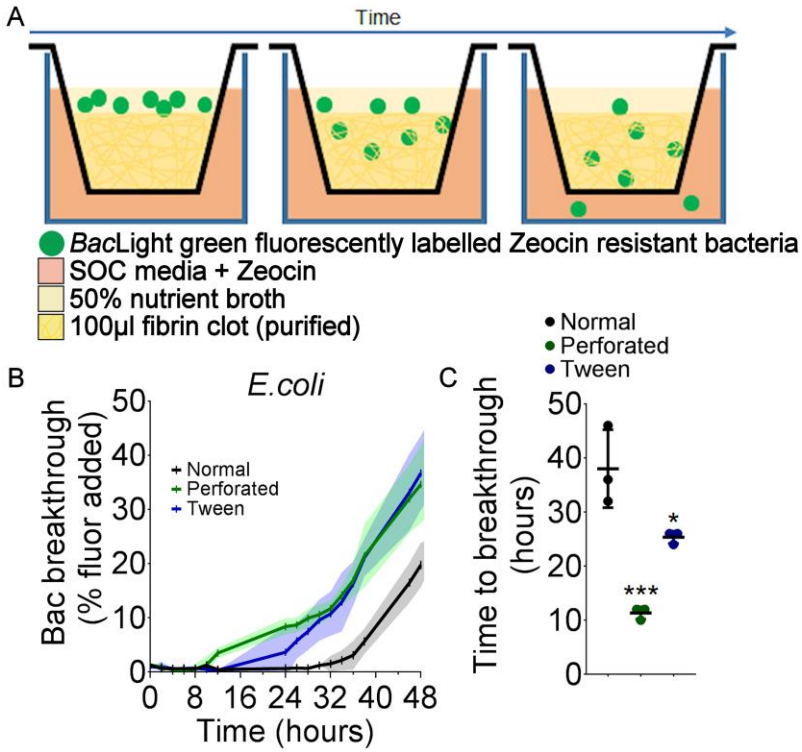

Figure. 5. Fibrin film slows bacteria movement through clot. **A,** Diagrammatic representation of the bacteria clot migration assay in the Boyden chamber. Bacteria moved from the 50% nutrient broth through the fibrin film (if present), into the fibrin clot and then into the super-optimal broth with 20 mM glucose (SOC) medium. Quantity of bacteria moving through the clot over time was analysed by fluorescence in the SOC media. **B,** Movement of fluorescently labelled *E.coli* bacteria through the clots (displayed as quantity of fluorescent bacteria breaking through the clot as a percentage of fluorescent bacteria added) with three different film conditions; normal, perforated or removal with tween-20. **C,** Time taken for the first fluorescently labelled *E. coli* bacteria to break through the clot. * represents difference from normal clot. * $p<0.05$, *** $p<0.001$, n=3 experiments, one-way ANOVA, $F=29.29$, $df=2$, $p=0.0008$.

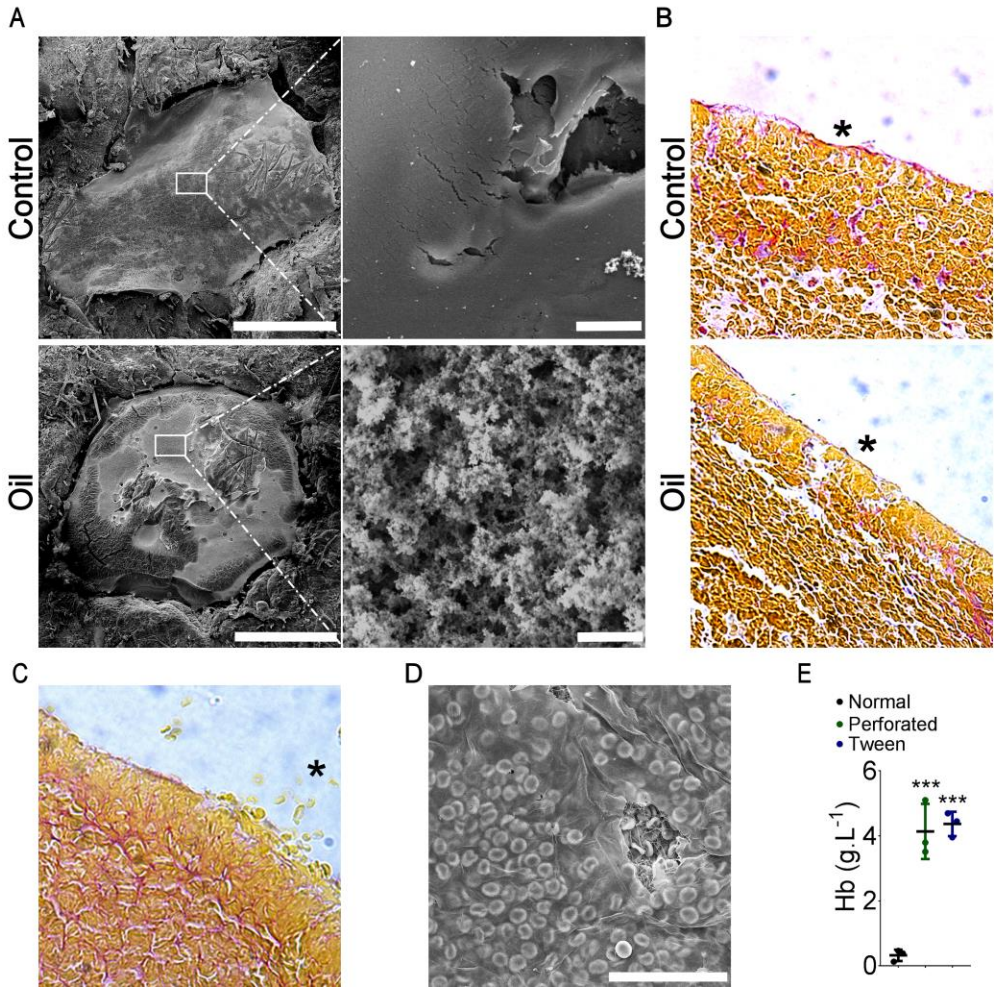

Figure. 6. Fibrin film formation in vivo. **A,** Clots were formed in a ventral, dermal puncture injury model in mice and left clear or covered with a layer of mineral oil, fixed, dehydrated and imaged by SEM. The white box represents the area of magnification for the image to the right. Clots covered with oil showed a rough fibrous clot surface, and clots left untreated showed a smooth fibrin film covering the clot. Images are representative of n=4 mice. Scale bars – left 1mm, right 2 μm **B,** Clots left clear or with a layer of oil covering the surface from the dermal puncture model were surgically removed, and cross-sections were stained with Martius, Scarlet and Blue (MSB; erythrocytes in yellow, and fibrin in pink). Fibrin film shows as continuous pink layer, clot appears yellow interspersed with pink. * highlight the air-liquid interface. Images representative of n=4 mice. **C,** Clots from the murine dermal puncture model covered with oil showed extrusion of red blood cells from the clot in the absence of a fibrin film. * highlights extrusion of red blood cells from the clot. Images representative of n=4 mice. **D,** Clots produced with human whole blood and thrombin, and imaged by SEM demonstrated containment red blood cells by the fibrin film. Images representative of n=3 individuals. Scale bar - 40μm. **E**, Haemoglobin retention assay in normal, perforated and tween-20 treated clots. * represents difference from normal clot. *** $p<0.001$, n=3 individuals, one-way ANOVA, $F=52.14$, $df=2$, $p=0.0002$. Hb – haemoglobin.

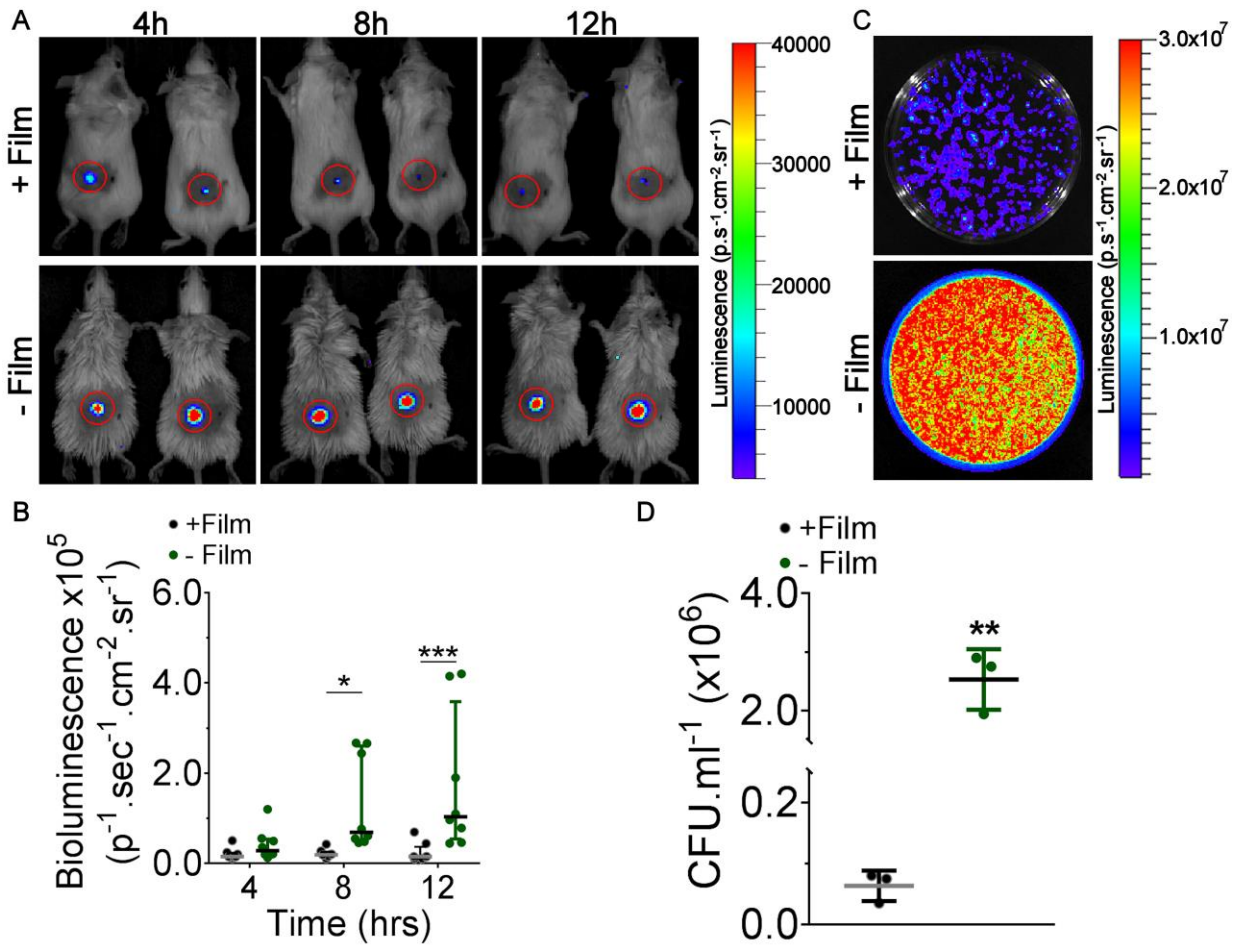

Figure. 7. Fibrin film slows bacteria proliferation and dissemination in vivo. **A,** Measurement of bioluminescent bacteria proliferation with or without film in a murine dermal injury model over time. Images representative of n=8 mice **B,** Quantification of bioluminescent bacteria in this model. * $p<0.05$, *** $p<0.001$, n=8 mice, Kruskal-Wallis test, Kruskal-Wallis statistic=36.55, 6 groups, p=<0.0001. **C**, Measurement of bioluminescent bacteria from wound and surrounding skin with and without film after 12h spread on agar plates. Images representative of n=3 mice **D**, CFU/ml of bacteria from wound and surrounding skin with or without film after 12h. ** $p<0.01$, n=3 mice, Unpaired t-test, t=8.26, df=4, p=0.0012. CFU – colony forming unit.